아연과 인듐이 첨가된 은-팔라디움 합금의 석출에 의한 시효경화기구**

김형일, 김성민, 전병욱, 조수연, 이광영, 권용훈, 설효정*

부산대학교 치의학전문대학원 치과재료학교실 및 중개치의학연구소

Age-hardening mechanism by precipitation in a zinc- and indium-added silver-palladium alloy**

Hyung-Il Kim, Sung-Min Kim, Byung-Wook Jeon, Su-Yoen Cho, Gwang-Young Lee, Yong Hoon Kwon, Hyo-Joung Seol*

Department of Dental Materials, Institute of Translational Dental Sciences, School of Dentistry, Pusan National University, Beomeo-Ri, Mulgeum-Eup, Yangsan-Si, Gyeongsangnam-Do, 626-814, South Korea

(Received: Feb. 4, 2014; Revised: Feb. 13, 2014; Accepted: Feb. 13, 2014)

DOI : http://dx.doi.org/10.14815/kjdm.2014.41.1.39

ABSTRACT

The age-hardening mechanism of a copper-free silver-palladium alloy is unclear yet because the age-hardening mechanism is variable even with slight compositional changes. The aim of present study is to elucidate the age-hardening mechanism and relation of age-hardenability with the phase transformation and microstructural changes of a Zn- and In-added Ag-Pd alloy by means of the hardness test, X-ray diffraction study, field emission-scanning electron microscopic observation and energy dispersive spectrometer analysis. The matrix was composed of the Ag-rich α_1 phase containing small amounts of solute elements, and the particle-like structures were composed of the PdZn-based β_1 phase containing relatively large amounts of In. The lamellar-forming grain boundary reaction which is usually observed in Ag-Pd alloys containing Cu was not observed in the Zn- and In-added Ag-Pd alloy. The grain interior precipitate composed of the Pd-Zn-rich phase containing In resulted in apparent hardening from the early stage of aging process, and its coarsening by prolonged aging resulted in softening. In the specimen alloy, Zn and In formed extra phase preferentially with Pd, and the amount of Zn and In which took part in the precipitation hardening was very small.

Key words: Age-hardenability; Precipitation; Zn and In-added Ag-Pd alloy; Softening; microstructural change

INTRODUCTION

Dental silver-palladium alloy for crown and bridge fabrication belongs to the alternative alloy for dental gold alloy due to the economic reason. Such a dental silver-palladium alloy is designed to have an age-hardenability as sufficient as dental gold alloy. In silver-palladium system, silver and palladium has no miscibility limit for each other, and thus shows no age-hardenability without a proper hardener such as copper (Massalski, 1990). Copper has miscibility limit with silver, and thus shows an age-hardenability by precipitation of copper from the silver-rich matrix (Kanzawa et al., 1963; Yasuda, 1969; Ohta et al., 1975; Ohta et al., 1979; Niemi et al., 1984; Massalski, 1990, Seol et al., 2005a; Seol et al., 2005b; Seol et al., 2006; Yu et al., 2008,). However, in such a copper-added silver-palladium alloy, copper tends to form stable phases preferentially with palladium, and thus only the rest copper which exists as a solute takes part in the hardening mechanism. The preferentially

* 교신저자 : 설효정, 부산대학교 치의학전문대학원 치과재료학교실 및 중개치의학연구소, Tel: 051-510-8229, E-mail: seol222@pusan.ac.kr

** 이 논문은 부산대학교 자유과제 학술연구비(2년)에 의하여 연구되었음

formed extra phases composed of copper and palladium are disadvantageous from the viewpoint of corrosion resistance because the multi-phase formation leads to preferential corrosion of electrochemically corrosion prone phase in the oral environment.

Recently, copper-free silver-palladium alloy is widely used (Suh and Lee, 2000; Lee et al., 2004). The age-hardening mechanism of such an alloy becomes different from that of the copper-containing silver-palladium alloy depending on the additives. In case of relatively large amounts of indium was added in copper-free silver-palladium alloy, most of indium exists as a dendrite or particle-like structure composed of the InPd phase, and thus, the rest indium content which exists as a solute in the matrix attributes to age-hardening by precipitating the In-rich phase (Lee et al., 2004). In case of relatively small amounts of indium was added in copper-free silver-palladium alloy, discontinuous precipitation of the Pd_3In-based phase attributed to age-hardening (Suh and Lee, 2000). In the present study, instead of copper, small amounts of zinc- and indium-added silver-palladium alloy was used. The age-hardening mechanism of such a copper-free silver-palladium alloy is unclear yet because the age-hardening mechanism is variable even with slight compositional changes. The aim of present study is to elucidate the age-hardening mechanism and relation of age-hardenability with the phase transformation and microstructural changes of a zinc- and indium-added silver-palladium alloy by means of the hardness test, X-ray diffraction study, field emission-scanning electron microscopic observation and energy dispersive spectrometer analysis.

2. Materials and method

2.1. Materials

The alloy used in this study was a dental silver-palladium alloy with white color (Aurolite CB, Aurium research, U.S.A.) for use as single units to short-span bridge fabrication, which belongs to a Type 2-3 alloy according to the ISO classification (ISO 22674:2006(E)). Table 1 lists the chemical composition of the alloy. The alloy samples were used in the form of small square pieces 8 mm × 8 mm × 1.5 mm in a rolled and annealed condition.

Table 1. Chemical composition of the alloy

Composition	Ag	Pd	In	Zn	Au	Ir
wt.%	69.6	23.97	3	2.4	1	0.03
at.%	68.8	24	2.75	3.9	0.53	0.02

2.2. Hardness test

Before the hardness tests, the alloy samples were solution-treated at 800°C for 10 min under an argon atmosphere, then quenched rapidly into iced brine to prevent any reactions. The samples were then aged isochronally in the temperature range of 300°C to 550°C, and were aged isothermally at 500°C for various times in a molten salt bath (25 wt.% KNO_3 + 30 wt.% KNO_2 + 25 wt.% $NaNO_3$ + 20 wt.% $NaNO_2$) which was used for the temperature range from 150°C to 550°C, and then quenched into ice brine for subsequent hardness testing. The hardness measurements were performed using a Vickers micro-hardness tester (MVK-H1, Akashi Co., Japan) with a 300 gf load and a dwell time of 10 s. All results were the average of five measurements.

2.3. X-ray diffraction (XRD) study

The XRD profiles were recorded on an X-ray diffractometer (XPERT-PRO, Philips, Netherlands) which was operated at 30 kV and 40 mA using Nickel-filtered Cu Kα radiation. The scanning rate of a goniometer was 2° (2θ/min). For the XRD study, powder specimens with a 300 mesh were produced by filing sample pieces. After being vacuum-sealed in a silica tube and solution-treated at 800°C for 10 min, they were isothermally aged at 500°C for various times in a molten salt bath, and then quenched into ice brine.

2.4. Field emission scanning electron microscopic (FE-SEM) observation

For FE-SEM observations, the plate-like samples were subjected to the required heat treatment, and prepared utilizing a standard metallographic technique. A freshly

prepared aqueous solution of 10 wt.% potassium cyanide (KCN) and 10 wt.% ammonium persulfate ($(NH_4)_2S_2O_8$) was utilized for the final etching of the samples. The specimens were examined at 15 kV by FE-SEM (JSM-6700F, JEOL, Japan).

2.5. Energy dispersive spectrometer (EDS) analysis

EDS analysis was performed to observe the distributional changes of each element in the specimen during the aging process. An EDS (INCA x-sight, Oxford Instruments Ltd., UK) attached to an FE-SEM (JSM-6700F, JEOL, Japan) was used at 15 kV to examine the plate-like specimens used for the FE-SEM observation.

3. Results and discussion

3.1. Age-hardening behavior

The plate-like specimens were aged isochronally in the temperature range of 300°C to 550°C to determine an appropriate aging temperature for the specimen. Figure 1 shows the isochronal age-hardening curves of the specimen solution-treated at 800°C for 10 min, and then aged in the temperature range of 300°C to 550°C for 10 min and 20 min. The specimen showed an apparent age-hardenability at 500°C. This indicated that the driving force for atomic diffusion related to precipitation was maximum at the aging temperature of 500°C. Therefore, the age-hardening behavior was observed at 500°C.

Figure 2 presents the isothermal age-hardening curve of the specimen solution-treated at 800°C for 10 min and aged at 500°C. The hardness increased apparently and constantly without an incubation period until 20 min to the maximum value (192.4 HV). Thus, the precipitation hardening was expected from the early stage of aging process in the specimen alloy. This value was apparently lower than the maximum hardness value (285 HV) which was obtained in the Ag-Pd alloy containing Cu (Kim et al., 2007). The maximum hardness was maintained until 50 min. Then, the hardness decreased constantly until 20,000 min.

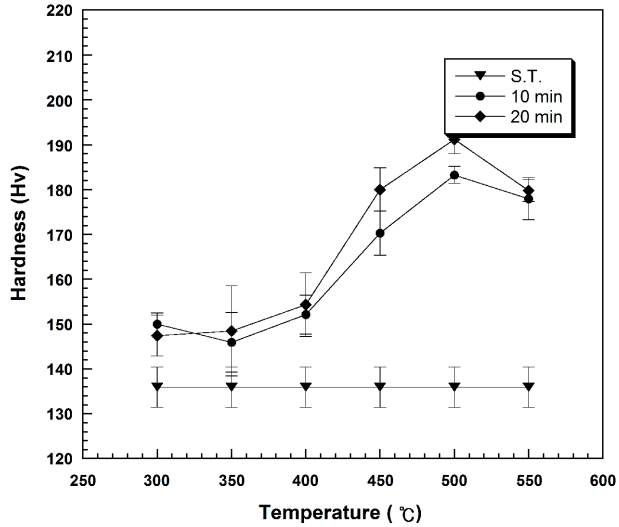

Fig. 1. Isochronal age-hardening curves of subject alloy aged in temperature range of 300-550° C for 10 and 20 min.

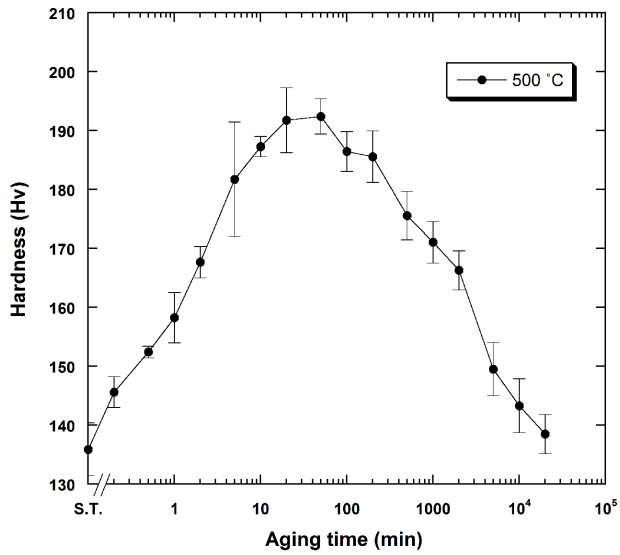

Fig. 2. Isothermal age-hardening curve of subject alloy aged at 500° C.

3.2. Phase transformation

To characterize the phase transformation mechanism which is related to age-hardenability, the XRD study with aging time was done. Figure 3 shows the changes in the XRD pattern during isothermal aging at 500°C. The solution-treated specimen had two phases of face centered cubic (f.c.c.) structure with a lattice parameter of a_{200}=0.4049 nm (α_1) and face centered tetragonal (f.c.t.) structure of AuCu-ordered type with lattice parameters of a_{200}=0.4182 nm and c_{111}=0.3495 nm (β_1). By considering the lattice parameters together with the

alloy composition, the f.c.c. α_1 phase and the f.c.t. β_1 phase were supposed to be the Ag-rich phase and the PdZn-based phase, respectively. The lattice parameters of the PdZn phase were reported to be a=0.41 nm and c=0.3295 nm, and which are slightly smaller than those obtained in the present study (Villars and Calvert, 1985). From such a fact, the β_1 phase was supposed to contain In which has relatively larger atomic size than Pd and Zn (Cullity, 1978). This will be further discussed in EDS analysis.

By prolonged aging the solution-treated specimen at 500°C, slight changes were observed in the diffraction peak position of the Ag-rich α_1 phase and the PdZn-based β_1 phase, even though there was no newly appeared diffraction peak. The f.c.c. 200 α_1 peak shifted slightly to the lower diffraction angle side. And the 200 β_1 peak shifted to the higher diffraction angle side without changes in the 111 β_1 peak position. Thus, by aging the specimen at 500°C for 20,000 min, the lattice parameter, a of the Ag-rich α_1 phase slightly increased to a_{200}=0.4052 nm (α_1' phase), and the lattice parameters, a and c of the PdZn-based β_1 phase slightly decreased to a_{200}=0.4164 nm and slightly increased to c_{111}=0.3513 nm, respectively (β_1' phase).

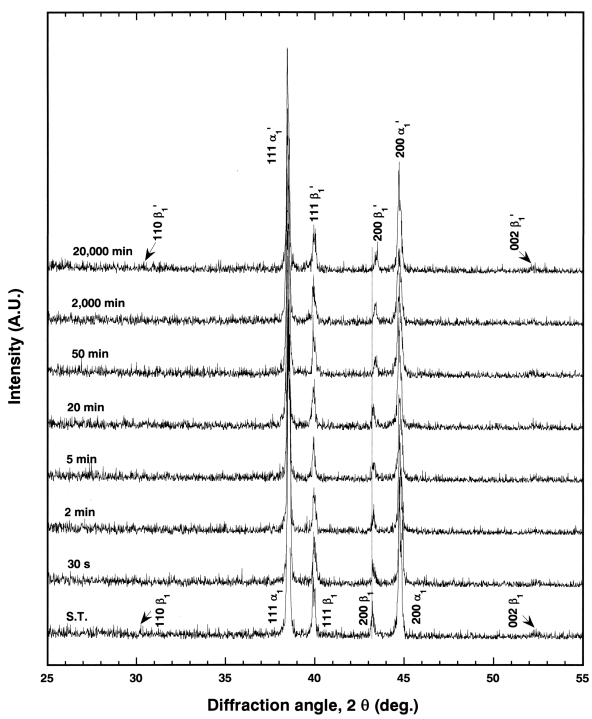

Fig. 3. *Variations of the XRD pattern during the isothermal aging at 500° C with aging time.*

3.3. Microstructural changes

Microstructural changes related to the age-hardenability was observed by FE-SEM. Figure 4 shows FE-SEM micrographs at a magnification of 3000× (1) and 20,000× (2) for the specimens solution-treated at 800°C for 10 min (a) and aged at 500°C for 20 min (b), 50 min (c), 500 min (d) and 20,000 min (e). The solution-treated specimen (a) showed matrix and particle-like structures of micro and nano sizes. By considering the corresponding XRD results which showed the two phases of the major Ag-rich phase (α_1) and the minor PdZn-based phase (β_1) in the solution-treated state, it was thought that the matrix was composed of the Ag-rich α_1 phase, and the particle-like structures of various sizes were composed of the PdZn-based β_1 phase. In the specimen aged for 20 min (b) when the maximum hardness value (192 Hv) was obtained, fine precipitates were observed in the entire grain interior. On the other hand, such fine precipitates were not found in the grain boundary and the particle-like structures of various sizes. In the further aged specimen until 50 min (c) when the maximum hardness value was maintained, the microstructure was similar to that of the specimen aged for 20 min. And the lamellar-forming grain boundary reaction which is usually observed in Ag-Pd alloys containing Cu was not observed (Kawashima et al., 1991). In the corresponding XRD pattern, the 200 peak of the PdZn-based β_1 phase shifted to higher diffraction angle side, indicating the decrease in lattice constant, a. Thus, atomic diffusion of some ingredients was thought to have occurred in the particle-like structures along the boundaries. In the specimen aged for 500 min (c) when the hardness decreased to 176 (Hv), the fine precipitates which covered the grain interior became coarse slightly. By overaging the specimen until 20,000 min (e) when the hardness decreased apparently, the grain interior precipitates grew to be indiscernible from the particle-like structures of nano-size. And there was no apparent microstructural change in particle-like structures. From the above, it is clear that the grain interior precipitation resulted in hardening from the early stage of aging process, and its coarsening by prolonged aging resulted in softening. The interfaces

between the grain interior precipitates and the solute-depleted matrix contain large amounts of lattice strains by the gap in the lattice parameter between the Ag-rich α_1' phase and the PdZn-based β_1' phase. Thus, the reduction of interfaces by microstructural coarsening resulted in apparent softening (Hisatsune et al., 1991; Kim et al., 1999; Lee et al., 2004).

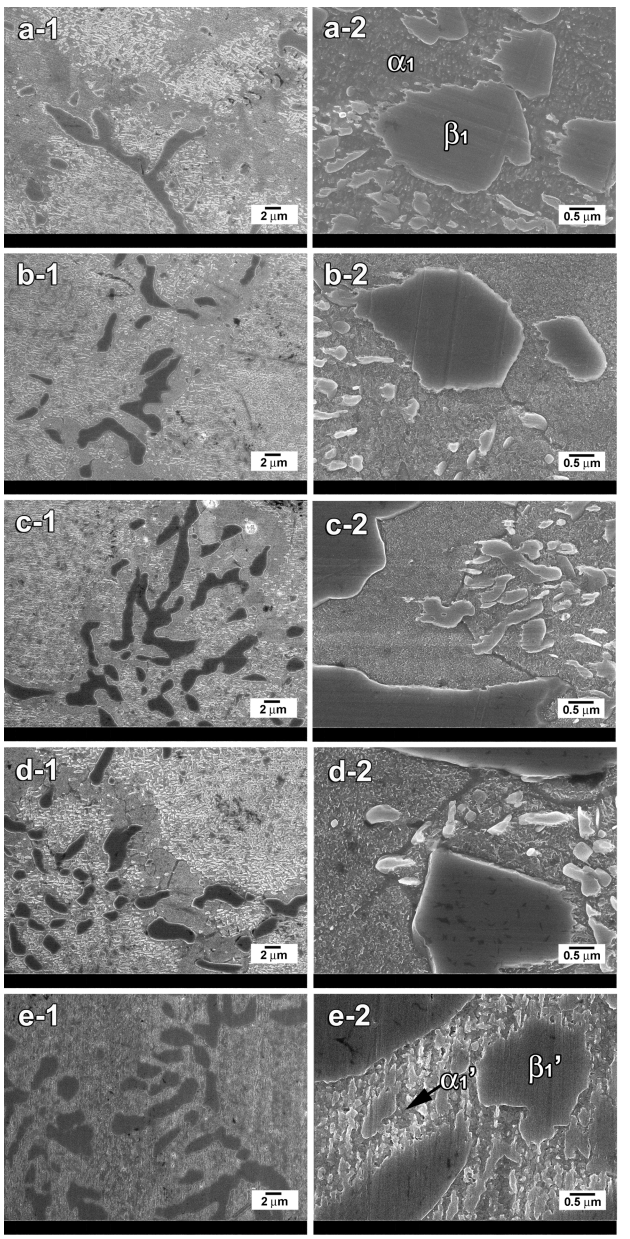

Fig. 4. *FE-SEM micrographs at a magnification of 3000× (1) and 20,000× (2) for the specimens solution-treated at 800° C for 10 min (a) and aged at 500° C for 20 min (b), 50 min (c), 500 min (d) and 20,000 min (e).*

3.4. Elemental distribution

EDS analysis was done to examine the elemental distribution in the matrix and particle-like structures with aging time. Figure 5 shows FE-SEM micrographs of the specimen solution-treated at 800°C for 10 min (a), and aged at 500°C for 20,000 min (b). The elemental distribution in the matrix (m), particle-like structures (p), matrix covered by precipitates (m+ppt) was analyzed by EDS, and the results were listed in Table 2. In the matrix (m) regions of the solution-treated specimen (Fig. 5-a), Ag increased apparently, and Pd, Zn and In decreased compared to the alloy composition listed in Table 1. In the particle-like structures (p) of the solution-treated specimen (Fig. 5-a), the opposite was observed. Especially, Zn was extremely concentrated in the particle-like structures. In the specimen aged at 500°C for 20,000 min (Fig. 5-b), the elemental distribution in the particle-like structures (p) was similar to that of the solution-treated specimen. In the matrix covered by precipitates (m+ppt), the content of Pd, Zn and In increased compared to that in the matrix (m) regions of the solution-treated specimen (Fig. 5-a). This indicated that the precipitates were possibly composed of the Pd-Zn-rich phase containing In.

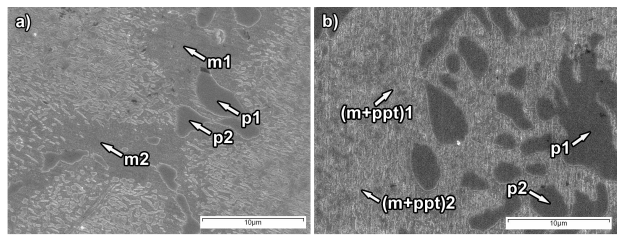

Fig. 5. *FE-SEM micrographs of the specimen solution-treated at 800° C for 10 min (a), and aged at 500° C for 20,000 min (b).*

By considering the results of elemental distribution together with the XRD results, it is clear that the matrix was composed of the Ag-rich α_1 phase containing small amounts of solute elements. The particle-like structures were composed of the PdZn-based β_1 phase containing relatively large amounts of In. In Ag-Pd system, Ag and Pd has no miscibility limit for each other, and thus shows no age-hardenability without proper hardener (Massalski, 1990). In the present study with Zn and In-added Ag-Pd

Table 2. EDS analysis at the regions marked in Fig. 5

Region (at%)		Zn	Pd	Ag	In	Au	Ir
a	p1	24.82	51.52	14.58	8.53	0.43	0.12
a	p2	26.04	52.17	13.31	8.11	0.37	0
a	m1	1.51	12.36	83.69	1.61	0.84	0
a	m2	0.75	9.61	87.81	0.73	1.1	0
b	p1	27.57	52.86	11.77	7.8	0	0
b	p2	26.96	52.41	12.98	7.65	0	0
b	(m+ppt)1	4.70	29.97	62.16	3.16	0	0
b	(m+ppt)2	3.5	22.88	70.64	2.98	0	0

alloy, precipitation of the Pd-Zn-rich phase containing In resulted in apparent hardening. But, Zn and In formed extra phase preferentially with Pd, and the amount of Zn and In which took part in the precipitation hardening was very small. Thus, it is recommanded that the addition of Zn and In is better to be restricted to minimum in Ag-Pd alloy to prohibite the extra phase formation.

4. Conclusions

Age-hardening mechanism and relation of age-hardenability with the phase transformation and microstructural changes of a Zn- and In-added Ag-Pd alloy were examined by means of the hardness test, X-ray diffraction study, field emission-scanning electron microscopic observation and energy dispersive spectrometer analysis. The results are as follows.

1. The matrix was composed of the Ag-rich α_1 phase containing small amounts of solute elements, and the particle-like structures were composed of the PdZn-based β_1 phase containing relatively large amounts of In.
2. The grain interior precipitate composed of the Pd-Zn-rich phase containing In resulted in apparent hardening from the early stage of aging process, and its coarsening by prolonged aging resulted in softening.
3. In the specimen alloy, Zn and In formed extra phase preferentially with Pd, and the amount of Zn and In which took part in the precipitation hardening was very small.

References

Cullity BD (1978). Elements of X-ray diffraction. 2nd ed. Addison-Wesley publishing Co. Inc Massachusetts pp. 506-507.

Hisatsune K, Udoh KI, Sosrosoedirdjo BI, Tani T, Yasuda K (1991). Age-hardening characteristics in an AuCu-14at.% Ag alloy. *J Alloys Compd* 176: 269-283.

Kanazawa Y, Uzuka T, Kondo E, Shoji M (1963). Study on the Ag-Pd alloy. *J Jpn Soc Dent Appar Mater* 4:157-160.

Kawashima I, Araki Y, Ohno H (1991). Retardation of grain boundary reactions in Ag-Pd-Cu alloys by additions of small amounts of other elements. *J Mater Sci* 26:1113-1118.

Kim HI, Jang MI, Kim MS (1999). Age-hardening associated with grain boundary precipitation in a commercial dental gold alloy. *J Oral Rehabil* 26: 215-222.

Kim HI, Jeon GH, Yi SJ, Kwon YH, Seol HJ (2007). Hardening and overaging mechanism of a commercial Au-Ag-Cu-Pd dental alloy. *J Alloys Compd* 441:124-130.

Lee HK, Moon HM, Seol HJ, LeeJE, Kim HI (2004). Age hardening by dendrite growth in a low-gold dental casting alloy. *Biomaterials.* 25:3869-3875.

Massalski TB (1990). Binary alloy phase diagrams, 2nd ed., ASM International, Materials Park, pp. 72-74 (Ag-Pd), 28-29 (Ag-Cu).

Niemi L, Hero H (1984). The structural of a commercial dental Ag-Pd-Cu-Au casting alloy. *J Den res* 63:149-154.

Ohta M, Hisatsune K, Yamane M (1975). Study on the

age-hardenable silver alloy. III: On the aging Precess of dental Ag-Pd-Cu-Au alloy. *J Jpn Soc Dent Appar Mater* 16:144-149.

Ohta M, Hisatsune K, Yamane M (1979). Age Hardening of Ag-Pd-Cu dental alloy. *J Less-Common Met* 65:11-21.

Seol HJ, Kim GC, Son KH, Kwon YH, Kim HI (2005a). Hardening mechanism of an Ag-Pd-Cu-Au dental casting alloy. *J Alloys Compd* 387:139-146.

Seol HJ, Lee DH, Lee HK, Takada Y, Okuno O, Kwon YH, Kim HI (2006). Age-hardening and related phase transformation in an experimental Ag-Cu-Pd-Au alloy. *J Alloy Compd* 407:182-187.

Seol HJ, Park YG, Kwon YH, Takada Y, Kim HI (2005b). Age-hardening behaviour and microstructure of a silver with high Cu content for dental application. *J Mater Sci* 16:977-983.

Suh YC, Lee ZH (2000). Precipitation behavior of Ag-Pd-In dental alloys. *J Mater Sci Mater Med* 11: 43-48.

Villars P, Calvert L D (1985). Pearson`s Handbook of Crystallographic Data for Intermetallic phases. p. 3026.

Yasuda K (1969). Study on the age-hardenability of dental precious metal alloy. *J Jpn Soc Dent Appar Mater* 10:156-166.

Yu CH, Park MG, Kwon YH, Seol HJ, Kim HI (2008). Phase transformation and microstructural changes during aging process of an Ag-Pd-Cu-Au alloy. *J alloys Compd* 460:331-336.